Scavenging dicarbonyls with 5'-O-pentyl-pyridoxamine improves insulin sensitivity and reduces atherosclerosis through modulating inflammatory Ly6C^{hi} monocytosis and macrophage polarization

Jiansheng Huang[1], Patricia G. Yancey[1], Linda S. May-Zhang[2], Huan Tao[1], Youmin Zhang[1], Lei Ding[1], John A. Oates[1,2], Venkataraman Amarnath[3], L. Jackson Roberts II[2], Sean S. Davies[2], MacRae F. Linton[1,2]

[1]Department of Medicine, Atherosclerosis Research Unit, Vanderbilt University Medical Center, Nashville, TN

[2]Department of Pharmacology, Vanderbilt University, Nashville, TN

[3]Department of Pathology, Microbiology & Immunology, Vanderbilt University Medical Center, Nashville, TN

Address correspondence to:
MacRae F. Linton, MD
2220 Pierce Avenue, Nashville, TN
Department of Cardiovascular Medicine, Atherosclerosis Research Unit
Vanderbilt University Medical Center
Email: macrae.linton@vanderbilt.edu

Short title: 5'-O-pentyl-pyridoxamine improves insulin sensitivity and reduces atherosclerosis

Background: Lipid peroxidation products impair HDL function and contribute to the development of atherosclerosis. Ours and other studies have shown that reactive dicarbonyls such as Isolevuglandins (IsoLG) and malondialdehyde (MDA), crosslink apoAI and impair the ability of HDL to promote cholesterol efflux. We examined whether scavenging of reactive dicarbonyls protects against the development of insulin resistance and atherosclerosis.

Methods and Results: Here, we found that 5'-O-pentyl-pyridoxamine (PPM), a potent scavenger of reactive dicarbonyls, abolished MDA-mediated crosslinking of apoAI in HDL by 80 % ($P<0.05$). In addition, PPM prevented the reduction in cholesterol efflux capacity of MDA treated HDL and preserved the cholesterol efflux capacity of MPO-modified HDL in *Apoe*$^{-/-}$ macrophages. Furthermore, PPM significantly improved the cholesterol efflux capacity and PON1 activity of HDL in *Ldlr*$^{-/-}$ mice ($P<0.05$), indicating that PPM protects HDL from modifications by reactive dicarbonyls and maintains HDL function in vivo. Importantly, PPM improved hyperglycemia and insulin sensitivity in male *Ldlr*$^{-/-}$ mice. Administration of 1 mg/mL of PPM, versus 1 mg/mL of the nonreactive analogue PPO, to *Ldlr*$^{-/-}$ mice consuming a western diet (WD) for 16 weeks reduced the extent of proximal aortic atherosclerosis by 48% and by 46% ($P<0.05$) in female and male *Ldlr*$^{-/-}$ mice. PPM also reduced the extent of en face aortic lesion by 52% in male *Ldlr*$^{-/-}$ mice. In addition, PPM reduced pro-inflammatory enzyme MPO expression by 57.5% and the number of TUNEL positive cells by 52% ($P<0.01$) in atherosclerotic lesions of *Ldlr*$^{-/-}$ mice. Immunohistochemistry studies revealed that PPM reduced the lesion macrophage content by 55% ($P<0.05$). Importantly, PPM increased M2 marker Arg1+ in macrophages of lesions and reduced the number of blood pro-inflammatory Ly6C^{hi} monocytes and the ratio between Ly6C^{hi} and Ly6C^{low}, but not the numbers of Ly6C^{low}, neutrophils in *Ldlr*$^{-/-}$ mice. Similarly, treatment of *Apoe*$^{-/-}$ mice on a WD for 16 weeks with PPM significantly reduced the extent of atherosclerotic lesions and also enhanced plaque stability as evidenced by a 47% increase in fibrous cap thickness and a 64.7% reduction in necrotic core area.

Conclusions: Reactive dicarbonyl scavenging with PPM in vivo preserves HDL function which improves insulin sensitivity and decreases atherosclerosis development. These results support the therapeutic potential of reactive dicarbonyl scavenging in the treatment of insulin resistance and atherosclerotic cardiovascular disease.

Keywords: Cholesterol efflux, high-density lipoprotein (HDL), malondialdehyde (MDA), macrophage, myeloperoxidase (MPO), 5'-O-pentyl-pyridoxamine (PPM).

Introduction

Atherosclerosis is a systemic inflammatory disorder that initiates early in life and continuously builds up throughout the arterial wall over decades. Clinical and mechanistic studies have shown that many factors that facilitate the development of atherosclerosis, presenting potential targets for therapeutic modification. Although clinical trials of lowering atherogenic lipoproteins LDL-C have been demonstrated to reduce cardiovascular events, a considerable residual risk of cardiovascular disease still exists [1, 2]. This highlights the need to find novel therapeutic approaches to targeting atherosclerosis to achieve more effective reductions in cardiovascular risk.

Pleotropic functions of HDL, including anti-inflammatory function and mediation of reverse cholesterol transport are central in protecting against cardiovascular disease [3]. Cholesterol efflux capacity, a measure of HDL function in the first step of RCT, was reported to be inversely associated with measures of cardiovascular events, independent of HDL-C levels [4-6]. Recent observations support the concept that qualitative changes in HDL composition promote its atheroprotective functions [7]. HDL is also identified as an important target for treatment of type 2 diabetes (T2D) which increases atherosclerosis development. HDL promotes the uptake of glucose in skeletal muscle and increases the synthesis and secretion of insulin from pancreatic β cells and thus may have beneficial effects on glycemic control [8, 9]. Clinical studies found that reconstituted HDL increased plasma insulin and decreased plasma glucose in patients with T2D by activating AMP-activated protein kinase (AMPK) [9, 10]. Cholesteryl ester transfer protein (CETP) inhibitor torcetrapib has been shown to improve insulin sensitivity in patients with type 2 diabetes [11].Thus, mounting evidence demonstrates HDL function is crucial in chronic inflammatory disorders, such as T2D and atherosclerosis.

Studies have shown that myeloperoxidase (MPO) promotes the formation of dysfunctional HDL and there is abundant of dysfunctional HDL in human atherosclerosis [12, 13]. Several reactive dicarbonyls including malondialdehyde (MDA), 4-oxo-nonenal, and isolevuglandins (IsoLG) are endogenously formed during lipid peroxidation. Immunization with MDA epitopes leads to atheroprotection in mouse and rabbit models [14, 15], which highlights the importance of MDA epitopes in atherosclerosis. Synthetic MDA-lysine can promote monocyte activation and vascular complications via induction of inflammatory pathways [16]. Modifying apoAI by MDA blocks cholesterol efflux from macrophages [17]. In addition, dysfunctional apoAI is present in human atherosclerotic lesions[13] including MDA modified HDL [17]. In addition, our recent studies showed that IsoLG modification of HDL reduces the cholesterol efflux and anti-inflammatory capacity [18]. Importantly, HDL from familial hypercholesterolemic (FH) versus control subjects contains significantly more IsoLG adducts which likely contribute to the dysfunctional FH-HDL [18]. Taken together, mounting evidence supports the concept that HDL atheroprotective function can be impaired and that reactive dicarbonyls such as MDA and IsoLG, contribute to HDL dysfunction, insulin resistance, and the development of atherosclerosis.

In the current studies, we utilized a potent reactive dicarbonyl scavenger, 5'-O-pentyl-pyridoxamine (PPM), to dissect the role of reactive carbonyl species in causing HDL dysfunction in promoting the development of insulin resistance and atherosclerosis. Our earlier studies demonstrated that the PPM versus lysine residues reacts nearly 2000 times faster with the reactive dicarbonyl, IsoLG, thereby preventing lysine modification[19]. We found that scavenging reactive dicarbonyls with PPM prevents MPO-mediated impairment of HDL cholesterol efflux capacity in vitro, and importantly, in vivo administration of PPM to hypercholesterolemic mice increased HDL cholesterol efflux capacity and PON1 activity without affecting plasma cholesterol levels. Consistent with the effects on HDL function, administration of PPM to *Ldlr*$^{-/-}$ mice consuming a western diet reduced insulin resistance, atherosclerotic

lesion extent, lesion M1 macrophages, blood Ly6C^{hi} monocytes, and lesion TUNEL positive macrophages. Furthermore, PPM treatment increased the plaque fibrous cap thickness and reduced the necrotic area thereby improving plaque stability. Taken together, our results suggest that reactive dicarbonyl scavenging has high therapeutic potential in preventing HDL dysfunction, insulin resistance, and atherosclerosis development.

Material and Methods

Mice — *Apoe*$^{-/-}$ *and Ldlr*$^{-/-}$ mice were purchased from Jackson Laboratories (Bar Harbor, ME). Mice were maintained in micro-isolator cages with *ad libitum* access to a rodent chow diet containing 4.55 fat (PMI 5010, St. Louis, Mo) and water. The Institutional Animal Care and Use committee of Vanderbilt University approved mouse protocols. Experimental procedures and animal care were performed according to the regulations of Vanderbilt University's Institutional Animal Care and Usage Committee.

Reactive dicarbonyl scavengers — For animal studies, female and male *Ldlr*$^{-/-}$ mice on a western diet (WD) were treated with water alone or with either 1 g/L of PPM or the inactive analogue, pentylpyridoxine (PPO), for 16 weeks after pretreatment of mice on chow diet with PPM or PPO for 2 weeks, respectively. The effects of reactive dicarbonyl scavenging on atherosclerosis was also examined in male *Apoe*$^{-/-}$ mice that were on a WD and treated with water alone or with 1g/L of PPM for 16 weeks after pretreatment of the mice on a chow diet with water alone or PPM for 2 weeks.

Reagents — Fresh human HDL was isolated from normal subjects by sequential density ultracentrifugation as previously described [18]. Maloncarbonyl bis-(dimethylacetal) and H_2O_2 were purchased from Sigma-Aldrich (St. Louis, MO). EnzCheck PON1 activity kit was purchased from Invitrogen (Carlsbad, CA). The chemiluminescent Western Lightning ultra-

reagent was obtained from PerkinElmer Inc. (Waltham, MA). Primary antibody apoAI was purchased from Meridian Life science (Memphis, TN). Primary anti-MOMA2 and anti-CCR2 antibodies were purchased from BioRad and Biolegend, respectively. Secondary antibody HRP conjugated- rabbit anti-goat IgG and primary MPO antibody were purchased from Sigma-Aldrich (St. Louis, MO). Arg1 antibody was purchased from R&D. Secondary fluorescent antibodies were obtained from BioLegend. Pentyl-pyridoxine (PPO), and 5'-O-pentyl-pyridoxamine (PPM) were easily solubilized in water and prepared as a 100 mM stock and stored as small aliquots in -80ºC until use. Fresh working solutions were prepared before each assay and diluted in water to the appropriate concentrations.

Effect of PPM on modification of HDL with MDA — HDL modification with MDA was done in 50 mM phosphate buffer (pH 7.0) containing 100 μM DTPA. For the PPM inhibition reaction, 1 mM PPM or 5 mM PPM was incubated with 1mg/mL HDL for 10 min and then 0.25 mM MDA were added to initiate the reaction. The reactions were carried out at 37 °C for 24 h and stopped by dialysis against PBS overnight.

*Effect of PPM on modification of HDL with MP*O — The MPO-mediated HDL modification reactions were done in phosphate buffer (50 mM, pH 7.0) containing 100 μM DTPA, 1 mg/ml of HDL protein, 70 nM purified human MPO (A430/A280 ratio of 0.79), and 100 mM NaCl[20]. For the PPM inhibition reaction, 1 mM PPM was incubated with 1mg/mL HDL for 10 min and then 70 nM MPO, 160 μM H_2O_2, and 100 mM NaCl were added to initiate the reaction. The reactions were done at 37 °C for 1 h. In all reactions, working solutions of H_2O_2 were made fresh daily by diluting 30% H_2O_2 (BDH Chemicals, London, UK) according to the extinction coefficient for H_2O_2 at 240 nm, 39.4 $M^{-1}cm^{-1}$ [21]

Isolation of peritoneal macrophages — Peritoneal macrophages were isolated from 10 week-old

Apoe$^{-/-}$ mice 4 days after injection of 5% of thioglycollate. Peritoneal cells were collected by lavage using Ca^{2+} and Mg^{2+} free PBS and then centrifuged and re-suspended in DMEM containing 10% heat-inactivated FBS and 100 units/ml penicillin/streptomycin. Cells were plated onto 24-well culture plates ($1*10^6$ cells/well) and allowed to adhere for 2 h. Non-adherent cells were removed by washing two times with DPBS, and adherent macrophages were used for experiments.

Serum lipid measurements, lipid profiling of FPLC-separated lipoprotein fractions and ApoB-depleted serum preparation — Serum total cholesterol and triglyceride (TG) levels were measured by the enzyme-based method (Sigma) after overnight fasting. Lipid profiling of FPLC-separated lipoprotein fractions was done using gel filtration analysis with s Superose6 column on a Waters 600 FPLC system. 100µl of aliquot of mouse serum was injected onto the column and separated with a buffer containing 0.15 M NaCl, 0.01 M Na2HPO4, and 0.1mM EDTA (pH 7.5), at a flow rate of 0.5 mL/min. cholesterol levels were determined by the enzyme-based method (Sigma) after collecting the fractions [22]. ApoB-depleted serum was prepared as described [23, 24]. Briefly, to precipitate apoB-containing lipoproteins from serum, 400 µL of PEG 8,000 (20% in 200 mM glycine) was added to 1 ml serum, incubated for 15 min at room temperature, and then centrifuged at 1,900g for 20 min. The supernatant containing the apoB-depleted serum was collected and used for the cholesterol efflux experiments.

Measurement of PON1 activity— The PON1 activity was measured using the EnzCheck PON1 activity kit (Thermo Fisher Scientific). PON1 standards and diluted mouse serum samples were prepared in TSC buffer (20mM Tris-HCl, 150mM NaCl and 2mM $CaCl_2$, pH 8.0). The samples and standards were then incubated for 30 min with TSC buffer containing 100µM substrate. Fluorescence intensity was then measured using Biotek's Synergy MX Microplate reader

(Winooski, VT) with Gen 5 software at excitation wavelength of 368nm and an emission wavelength of 460nm after 30 min of incubation at 37 ^{0}C.

Measurement of HDL capacity to reduce macrophage cholesterol — To measure the capacity of HDL to reduce macrophage cholesterol content, *Apoe*$^{-/-}$ macrophages were isolated and incubated for 48 h with DMEM containing acetylated LDL (40 μg/ml). The cells were then washed and incubated for 24 h in DMEM supplemented with HEPES in the presence of 50 ug/mL human HDL, modified HDL, or 2.8% apoB-depleted serum. Cellular cholesterol was measured before and after incubation with cholesterol acceptor using an enzymatic cholesterol assay as described [25, 26].

Western blotting — Samples were incubated with β-mercaptoethanol and loading buffer for 10 min at 55 ^{0}C and then resolved by NuPAGE Bis-Tris electrophoresis using 4-12% gels for 1.5 h. The proteins were transferred onto PVDF membranes (Amersham Bioscience) at 150 V for 1.5 h. Membranes were blocked with 5% milk at room temperature for 2 h and incubated with primary goat antibodies specific to human apoAI overnight at 4 ^{o}C. The secondary antibodies conjugated with HRP were incubated with the membranes for 2 h at room temperature. Protein bands were visualized with ECL western blotting detection reagents (GE Healthcare) and quantified using ImageJ software (NIH).

Glucose tolerance test (GTT) and insulin tolerance test (ITT) — Insulin levels were measured by ELISA. For the GTT, mice were fasted for 4h, and 10 μL blood was taken from the tail vein for measurement of baseline levels. Mice were then injected with 1g/kg of glucose. Blood samples were taken at 15, 30, 45, 60, 90, 120 minutes after the glucose challenge and analyzed for blood glucose with a clinical meter [27]. For ITT, mice were fasted for 4h, and after taking a baseline blood sample, the mice were injected with insulin (0.5U/kg). Blood samples were then

taken at 15, 30, 60, 90, 120 minutes after insulin challenge and analyzed for blood glucose with a clinical meter [27]. The homeostatic model assessment for insulin resistance (HOMA-IR) was calculated using the equation fasting insulin (μU/ml) × fasting plasma glucose (mmol/liter)/22.5.

Measurement of atherosclerotic lesions — Aortas were flushed with PBS through the left ventricle and the entire aorta was dissected and en face was stained with Sudan IV as described. The extent of atherosclerosis was examined in Oil-Red-O stained cross-sections of the proximal aorta (15 alternate 10 μm cryosections for each mouse aorta). Images of the proximal and distal aorta lesions were analyzed using the KS300 imaging system (Kontron Electronik GmbH) [28].

HE staining of liver tissue— During dissection of the mice, livers were isolated, weighed, and stored for further analyses. After overnight fixation in 4% formaldehyde, tissues were embedded in paraffin, and 5 μm sections were collected and stained with hematoxylin & eosin (HE). Digital images were taken at a magnification of 200 using Olympus IX81 fluorescence microscope with SlideBook 6 (Intelligent-Image) software. The fat content of the liver was scored according to the content of fat droplets with the following scores: 0, no fat droplets; 1, very few fat droplets; 2, few fat droplets; 3, multiple fat droplets; and 4, many fat droplets [29].

Measurement of prostaglandin(PG) metabolites — Male LDLR-/- mice were given vehicle (n=8), 1 mg/mL PPM (n=8) for 8 weeks. Urine was collected for 6 hrs in metabolic cages with 2 mice per cage after 8 weeks of treatment with PPM and analyzed by GC/MS for 2,3-dinor-6-ketoPGF1 (2,3DN) and 11-dehydro TxB2 (11dTxB2) by the Eicosanoid Analysis Core at Vanderbilt University. The creatinine levels are measured using a kit (Enzo Life Sciences). The urinary metabolite levels in each sample are normalized using the urinary creatinine level of the sample and expressed in ng/mg creatinine.

Immunohistochemical (IHC) staining of atherosclerotic lesions — Immunofluorescence staining was used to examine protein levels in atherosclerotic lesions [28]. Briefly, 5 μm cross-sections of the proximal aorta were fixed in cold acetone (Sigma), blocked with 5% goat serum dilution (GSD), and incubated overnight at 4ºC with primary antibody to MOMA2, MPO, arginase 1 (Arg1), or C-C chemokine receptor2 (CCR2). After incubation for 1h at 37 ºC with the fluorescent labeled secondary antibody, the nuclei were stained with DAPI. The images were captured using an Olympus IX81 fluorescence microscope with SlideBook 6 (Intelligent-Image) software and quantified using ImageJ software (NIH).

Analysis of lesion apoptosis—The apoptotic cells in atherosclerotic lesion were measured by TUNEL staining of cross-sections of the proximal aorta. Briefly, 5 μm sections were fixed in 2% paraformaldehyde, treated with 3% citric acid, and then stained using the in situ TMR red cell death detection kit (Roche Applied Science). TUNEL-positive (TUNEL+) cells were counted in proximal aortic sections as described [28].

Masson's Trichrome staining— Masson's Trichrome staining procedure (Sigma) was used for measurement of lesion necrotic core size and fibrous cap thickness as previously described [30]. Briefly, 5 μm sections of the proximal aorta were fixed for 30 min with Bouin's solution and stained with hematoxylin for nuclei (black). Biebrich scarlet solution and phosphotungstic/phosphomolybdic acid were added to stain cytoplasm (red), and Aniline blue solution was applied to stain collagen (blue). Images were obtained and analyzed for fibrous cap thickness and % necrotic area using ImageJ software (NIH).

Flow analysis white blood cells — To measure the numbers of blood neutrophils, $Ly6C^{hi}$ monocytes, and $Ly6C^{low}$ monocytes in $Ldlr^{-/-}$ mice, blood cells were collected and stained with a

cocktail of antibodies targeting these cells [28]. Briefly, 100 μL of blood was collected using Natelson Blood collection tubes, and then incubated with Fc inhibitor CD16/32 for 10 min at RT. Lysis buffer (3 mL) was pre-warmed at 37 ^{o}C and added to the blood samples and incubated at room temperature for 30 mins to lyse red blood cells. Samples were centrifuged at 1200 rpm for 10 mins, and the cell pellets were re-suspended with 300 ul of FACS buffer (2% FBS in PBS). Antibodies against Ly6G (1A8, Biolegend), CD11b (M1/70, Biolegend), T cells (17A2, Biolegend), B cells (6D5, Biolegend) and monocytes subsets Ly6C (HK1.4, Biolegend) were added, and then incubated on ice for 45 min. Cells were washed with FACS buffer twice and analyzed using FACS DiVa v6.1 software (BD Biosciences) in the Research Flow Cytometry Core Laboratory, Veterans Administration Medical Center.

Statistics

The normality of the sample populations was examined by the Kolmogorov-Smirnov test. Differences between mean values were then determined by one-way ANOVA (Bonferroni's post-test), Kruskal-Wallis test (Bunn's multiple comparison), Mann-Whitney test, or Student's t-test using Graphpad Prism6. *P<0.05, **P<0.01, ***P<0.001.

Results

First, we examined the effects of PPM on MDA-mediated apoAI crosslinking and impairment of net cholesterol efflux capacity. Modification of HDL with 0.25 mM MDA increased the degree of apoAI crosslinking (Figures 1A and 1B) and decreased the capacity of the HDL to reduce macrophage cholesterol by 64% (Figure 1C). Addition of either 1 mM or 5 mM of PPM significantly decreased the MDA-mediated crosslinking of apoAI (Figures 1A and 1B) and improved the impairment of HDL net cholesterol efflux capacity (Figure 1C). In addition, MPO-mediated HDL modification reduced the net cholesterol efflux capacity by 54.5% and PPM (1 mM) prevented any impairment in cholesterol efflux (Figure 1D). More importantly,

administration of PPM to Ldlr$^{-/-}$ mice on a western diet increased the net cholesterol efflux capacity of HDL and enhanced the their HDL associated PON1 activity (Figures 1E and 1F).

Studies have shown that Ldlr$^{-/-}$ mice develop insulin resistance when consuming a WD which likely contributes to the development of atherosclerosis[31]. As PPM improves the function of HDL in *Ldlr*$^{-/-}$ mice (Figures 1E and 1F) which could impact insulin sensitivity, we next examined the effects of PPM on insulin resistance in *Ldlr*$^{-/-}$ mice. Consistent with other studies, the blood glucose and insulin levels which were measured after fasting overnight in male *Ldlr*$^{-/-}$ mice consuming a WD versus chow diet (CD) for 16 weeks. Administration of PPM to *Ldlr*$^{-/-}$ mice consuming a WD for 16 weeks reduced the fasting glucose and insulin levels (Figures 2A and 2B). The HOMA-IR levels as an indicator of insulin resistance shows that treatment with PPM reduced the HOMA-IR in *Ldlr*$^{-/-}$ mice on a WD to similar HOMA-IR values that were observed in Ldlr$^{-/-}$ mice consuming a chow diet (Figure 2C). To determine whether PPM improved insulin or glucose tolerance after 4hrs fasting, GTT and ITT were done after 12 weeks of male *Ldlr*$^{-/-}$ mice consuming a WD and being treated with PPM (Figures 2D-2G). Treatment of *Ldlr*$^{-/-}$ mice consuming a WD with PPM nearly normalized the dynamic change of glucose levels in response to glucose challenge and significantly decreased the glucose tolerance test area under the curve (AUC) (Figures 2D and 2E). Consistent with the GTT results, PPM reduced the dynamic changes of glucose levels in response to insulin challenge in male *Ldlr*$^{-/-}$ mice and significantly reduced the insulin tolerance test AUC (Figures 2F and 2G). More importantly, we found that PPM reduced the diet-induced fat deposition in the liver of male Ldlr-/- mice (Figure2H and 2I). Taken together, these results demonstrate that scavenging reactive dicarbonyls with PPM improves HDL function and reduces the western diet-induced moderate fat deposition in the liver and protects against insulin resistance in male *Ldlr*$^{-/-}$ mice.

To examine the effect of scavenging reactive dicarbonyls on atherosclerosis, female *Ldlr*$^{-/-}$ mice consuming a WD for 16 weeks and treated with water alone or containing PPM or its nonreactive analogue, PPO. As shown in Figures 3A-3C, PPM did not change the plasma cholesterol, TG levels, and lipid profiling of FPLC-separated lipoprotein fractions. Importantly, administration of PPM versus 1 mg/mL of the nonreactive analogue PPO, to *Ldlr*$^{-/-}$ mice consuming a WD reduced the extent of proximal aortic atherosclerosis by 48% ($P<0.05$) in female *Ldlr*$^{-/-}$ mice (Figures 3D & 3E). The extent of proximal aortic atherosclerosis was not significantly different PPO and water treated *Ldlr*$^{-/-}$ mice. In addition, immunohistochemistry analysis of macrophage MOMA2 shows that PPM versus PPO treatment reduced the lesion macrophage content by 55.6% (Figures 3F and 3G). Examination of the effects of reactive dicarbonyl scavenging on atherosclerosis revealed that similar to female *Ldlr*$^{-/-}$ mice, PPM treatment of male *Ldlr*$^{-/-}$ mice consuming a WD for 16 weeks reduced the extent of proximal aortic atherosclerosis by 46% ($P<0.05$) without affecting the plasma cholesterol and TG levels (Figures 4A-4D). In addition, PPM treatment reduced the en face aorta lesion content by 52% in male *Ldlr*$^{-/-}$ mice (Figures 4E and 4F). PPM also decreased the extent of proximal aortic atherosclerosis by 29% ($P<0.05$) in male *Apoe*$^{-/-}$ mice consuming the WD for 16 weeks (Supplemental Figures 1A, 1B and 1C). These results demonstrate that PPM treatment effectively decreases atherosclerosis development in experimental mouse models without changing plasma cholesterol and suggests that increased HDL function contributes to the impact on atherosclerosis.

As macrophage inflammation is modulated by HDL, we next examined the effects of scavenging reactive dicarbonyls on atherosclerotic lesion macrophage inflammatory markers. Immunohistochemical staining of the proximal aortic sections from male *Ldlr*$^{-/-}$ mice demonstrates that compared to water alone, PPM increased the number of anti-inflammatory Arg1 positive M2 macrophages by 120% (Figures 5A and 5B), and decreased the numbers of

pro-inflammatory CCR2 positive macrophages by 58% (Figures 5C and 5D). In addition, PPM treatment reduced the expression of proinflammatory, MPO by 58% (Figures 5E and 5F).

Consistent with reactive dicarbonyl scavenging reducing atherosclerotic lesion inflammation, PPM versus vehicle treatment decreased the number of apoptotic macrophages as evidenced by TUNEL staining in the proximal aortic lesion in *Ldlr*$^{-/-}$ mice (Figures 6A and 6B). PPM reduced the MDA-HDL, MDA-LDL content in these mice on WD for 16 weeks (Figure 6C and 6D). In consistent, PPM decreased the levels of MDA in lesions of *Ldlr*$^{-/-}$ mice (Figure 6E and 6F). Similar results were observed in male *Ldlr*$^{-/-}$ mice (Supplemental Figures 2A and 2B). PPM also reduced the inflammatory cytokine IL1β expression levels determined by ELISA (Figure 6G). Furthermore, examination of the effects on plaque necrosis and fibrous cap thickness demonstrates that PPM promotes plaque stability. Compared to vehicle, PPM decreased the necrotic area by 52.6% and increased the fibrous cap thickness by 41.7% in female *Ldlr*$^{-/-}$ mice (Figures 7A-7C). Similarly, PPM administration to *Apoe*$^{-/-}$ mice decreased the number of dead macrophages in the proximal aortic lesions by 60% (Supplemental Figures 1D and 1E). PPM treatment reduced the necrotic area by 64.7% and increased the fibrous cap thickness by 47% in the proximal aortic lesion of male *Apoe*$^{-/-}$ mice (Supplemental Figures 1F-1H). Importantly, treatment with PPM did not impact levels of urinary prostaglandin metabolites of prostacyclin, thromboxane, indicating that PPM does not result in significant inhibition of cyclooxygenase in mice in vivo (Supplemental Figure 4).

Studies have demonstrated that Ly6C^{hi} monocytes preferentially infiltrate the arterial wall and convert to M1 macrophages during inflammation thereby progressing the atheroma [32-34]. As HDL limits inflammatory Ly6C^{hi} monocytosis, we next examined the effects of reactive dicarbonyl scavenging on subsets of monocytes in female *Ldlr*$^{-/-}$ mice consuming a western diet for 14 weeks. Interestingly, we found that compared to water alone, PPM did not affect the

number of neutrophils, Ly6C ^{low} monocytes, T cells, or B cells, but markedly reduced the number of Ly6C^{hi} monocytes and the ratio of Ly6C ^{hi} to Ly6C ^{low} cells (Figures 8A-8F and Supplemental Figures 3A and 3B). Collectively, we demonstrate that scavenging reactive dicarbonyls improves HDL function, modulates macrophage polarization, represses Ly6C^{hi} monocytosis, and decreases lesion macrophage inflammation and death resulting in increased plaque stability.

Discussion

Studies implicate a role for lipid peroxidation in the development of atherosclerosis. While some studies administering antioxidants to humans showed decreased atherosclerosis, the majority of clinical trials have demonstrated no beneficial effect on cardiovascular events which may be due to the doses used or from impaired physiologic signaling by reactive oxygen species that could be atheroprotective. Lipid peroxidation produces highly reactive dicarbonyls including 4-oxo-nonenal, MDA, and IsoLG which covalently bind plasma/cellular proteins, phospholipids, and DNA resulting in altered function and toxicity. Our current studies demonstrate that reactive dicarbonyl scavenging with PPM effectively increased HDL atheroprotective functions and insulin sensitivity (Figure 1 & Figure 2), reduced the extent of atherosclerosis in hypercholesterolemic *LdlR*$^{-/-}$ and *Apoe*$^{-/-}$ mouse models (Figure 3, Figure 4 and Supplemental Figure 1). In addition, PPM administration and decreased monocytosis and plaque inflammation (Figure 5 & Figure 8). Importantly, reactive dicarbonyl scavenging enhanced plaque stability as substantiated by the increased fibrous cap thickness and the decreased necrotic core (Figure 6 & Figure 7). Thus, our studies suggest that reactive dicarbonyl scavenging with PPM has therapeutic potential to improve insulin sensitivity and reduce the risk of clinical events by decreasing atherosclerosis development and plaque instability.

To the best of our knowledge, this is the first experimental study of how rescuing HDL functionality rather than raising HDL-C levels improves insulin sensitivity and reduces atherosclerosis in hypercholesterolemic model. We found that PPM treatment reduces atherosclerosis development without changing plasma cholesterol levels (Figure 3 & 4) in hypercholesterolemic Ldlr$^{-/-}$ and Apoe$^{-/-}$ mice making it likely that the protection against atherosclerosis results from reactive dicarbonyl scavenging preserving normal molecular functions. HDL protects against atherosclerosis via a number of functions including mediating cholesterol efflux and preventing inflammation, and studies have demonstrated that markers of HDL dysfunction versus HDL-C levels are a better predictor of cardiovascular event risk[4-6]. Our recent studies showed that IsoLG modification of HDL reduces the cholesterol efflux and anti-inflammatory capacity and FH-HDL compared to control HDL contains more IsoLG-HDL adducts [18]. In addition, MDA modification of lipid-free apoAI impairs ABCA1 mediated cholesterol efflux and MDA-HDL adducts are present in human atherosclerotic lesions [17]. Consistent with these studies, we show that MDA modification of HDL promotes apoAI crosslinking and decreases it ability to mediate the net efflux of cholesterol from macrophage foam cells (Figures 1A-C). In addition, PPM treatment of *Ldlr*$^{-/-}$ mice decreased MDA content of HDL (Figure 6C). Importantly, our studies demonstrate that in vivo scavenging of reactive dicarbonyls with PPM increases HDL net cholesterol efflux capacity and PON1 activity (Figures 1) which likely contributes to the atheroprotective effects of reactive carbonyl scavenging in the setting hypercholesterolemia. Consistent with the increased HDL PON1 activity, reactive dicarbonyl scavenging with PPM decreased the MDA-LDL adducts in *Ldlr*$^{-/-}$ mice which also probably decreases atherosclerotic lesion formation (Figure 6D). Besides the atheroprotective effects of decreasing HDL dysfunction and LDL modification, reactive dicarbonyl scavenging likely acts directly in the arterial wall to reduce atherosclerosis as PPM decreased the MDA content of atherosclerotic lesions in *Ldlr*$^{-/-}$ mice (Figure 6).

Studies have demonstrated that Ly6C^{hi} monocytes dominate hypercholesterolemia-associated monocytosis in mice and give rise to inflammatory macrophages in the progressing atheroma [32]. In addition, infiltrating Ly6C^{hi} monocytes drive chronic, unresolved inflammation and impair tissue repair in mouse models of diabetes mellitus [35]. Furthermore, humans with hypercholesterolemia have increased numbers of CD14^{++}CD16^{+} monocytes (Ly6C^{hi} monocytes in mice) [36-39]. Importantly, there is growing evidence that Ly6C^{hi} monocytosis promotes plaque instability in humans. In a large clinical study of 951 patients undergoing elective coronary angiography, increased numbers of intermediate CD14^{++}CD16^{+} monocytes independently predicted cardiovascular death, myocardial infarction, and stroke [40]. Our finding that PPM reduces Ly6C^{hi} monocytosis in response to hypercholesterolemic stress provides a novel atheroprotective mechanism whereby dicarbonyl scavenging decreases atherosclerotic lesion formation and plaque destabilization without decreasing plasma cholesterol. It is likely that the effects of PPM on monocytosis are from dicarbonyl scavenging at level of hematopoietic stem/progenitor cells (HSPC). Studies have shown that hypercholesterolemia induces oxidative stress in HSPC causing enhanced p38 and Notch1 signaling resulting in markedly increased proliferation [41]. In addition, treatment of hypercholesterolemic Apoe$^{-/-}$ mice with antioxidants decreases HSPC proliferation [41]. It is also likely that the improvement in HDL function with PPM treatment contributes to the reduction in inflammatory monocytosis as HDL/apoAI reduces the proliferation of HSPC by mediating cholesterol efflux [42].

In the atherosclerotic lesions, inflammatory conditions induce the preferential conversion of infiltrating Ly6C^{hi} monocytes into proinflammatory M1 phenotype macrophages which are prominent in the progression of the atheroma and the development of unstable plaques [43]. Indeed, recent studies suggest that inflammation is a residual risk to cardiovascular disease as studies have shown that humans treated with the IL-1β monoclonal antibody, canakinumab, had a significantly lower rate of recurrent cardiovascular events which were independent of

cholesterol lowering [44]. Our studies show that reactive dicarbonyl scavenging reduced the IL-1β levels and decreased the number of inflammatory macrophages as evidenced by the reduced expression of MPO and CCR2 in Ldlr-/- mice(Figure 5 and Figure 6). Pharmacologic inhibition of MPO decreases atherosclerosis [45, 46] and MPO promotes plaque instability by modifying extracellular matrix protein, inhibiting NO availability, and reducing endothelial glycocalyx thickness [47-49]. CCR2 deficiency also reduces atherosclerosis [50], which is consistent with CCR2 being required for Ly6C^{hi} monocyte recruitment to atherosclerotic lesions. In addition, CCR2 expression on circulating monocytes is associated with vascular inflammation in humans at risk for cardiovascular disease [51]. Consistent with reactive dicarbonyl scavenging impacting monocyte infiltration, our studies show that mice treated with PPM had reduced numbers of macrophages in their atherosclerotic lesions (Figure 3). Also consistent with dicarbonyl scavenging reducing inflammation, PPM treatment increased the atherosclerotic lesion anti-inflammatory M2 macrophage content as evidenced by the increased Arg1 expression (Figure 5). Besides reactive dicarbonyl scavenging directly affecting macrophage inflammation, the enhanced HDL function induced by PPM treatment likely contributes to the increased lesional M1 to M2 macrophage phenotypic switch.

Studies have shown that HDL abrogates the induction of macrophages to an M1phenotype, as demonstrated by a reduction in the cell surface markers CD192 and CD64, as well as by decreased expression of MCP-1 (CCL2) [52]. HDL inhibits ERK1/2 and STAT3 phosphorylation in M1 macrophages [52]. HDL also increases expression of the M2 markers Arg1 and Fizz-1 via a mechanism requiring STAT6 [53]. It is worth noting that the effects of HDL on these signaling pathways in regulation of macrophage phenotype are intimately linked to its cholesterol efflux function [54, 55] which is enhanced by reactive dicarbonyl scavenging in vivo (Figure 1). Similar to other studies,[31] administration of a western diet to *Ldlr*$^{-/-}$ mice caused the development of insulin resistance. Interestingly, we found that reactive dicarbonyl scavenging improved insulin

sensitivity in the *Ldlr*$^{-/-}$ mice consuming a western diet (Figure 2). Evidence has mounted that HDL improves insulin resistance. Short term administration of reconstituted HDL into patients with T2D reduced fast glucose levels and improved glucose metabolism. In addition, HDL via its cholesterol efflux function reduces the fat deposition in the liver suggesting that the PPM effects on cholesterol efflux contributed to the improved insulin sensitivity [8, 9]. Furthermore, studies have shown that apoAI promotes activation of AMPK in skeletal muscle and liver which increases fatty acid β-oxidation and glucose uptake [9, 56]. To date, the apoAI receptor signaling pathways that operate in AMPK activation are unknown, but studies suggest that interaction with ABCA1 or SR-BI may be involved [57]. In this regard, both IsoLG- and MDA-apoAI adduct formation markedly reduce ABCA1 mediated efflux [13] [18], which requires apoAI interaction and signaling. In addition, oxidation of HDL alters interaction with SR-BI and severely impairs SR-BI signaling and function [58]. Oxidation of HDL also increases HDL internalization and apoAI degradation likely reducing apoAI function [59]. Taken together, it is plausible that reactive dicarbonyl scavenging rescues apoAI from degradation thereby preserving beneficial HDL/apoAI signaling pathways.

Understanding the mechanism through which scavenging reactive dicarbonyls improves insulin sensitivity and reduces atherosclerosis in hypercholesterolemic mice is of considerable importance. Our research shows that PPM prevents MPO mediated-HDL modification and MDA-HDL adduct formation. Importantly, treatment of hypercholesterolemic mice with PPM preserves HDL function in vivo. The atheroprotective effects of PPM also likely result from preventing dicarbonyl adduct formation with HSPC and intima cellular component as PPM reduces Ly6C^{hi} monocytosis and increases the number of lesional anti-inflammatory M2 macrophages. Consistent with PPM limiting atherosclerotic lesion inflammation, dicarbonyl scavenging reduced lesion cell death and necrosis thereby promoting plaque stability. As PPM treatment did not change plasma cholesterol levels and triglyceride levels, PPM offers a

therapeutic potential for solving the residual cardiovascular risk in patients treated with current LDL-C lowering medicine.

Acknowledgments and Sources of Funding

This work was supported by National Institutes of Health Grants: HL116263. Jiansheng Huang is supported by America Heart Association Postdoctoral Fellowship (19POST34450266). The analyses of urinary prostaglandin metabolites were performed in the Vanderbilt University Eicosanoid Core Laboratory.

References:

1. Linton, M.F., et al., *The Role of Lipids and Lipoproteins in Atherosclerosis*, in *Endotext*, L.J. De Groot, et al., Editors. 2016: South Dartmouth (MA).
2. Ridker, P.M., *Residual inflammatory risk: addressing the obverse side of the atherosclerosis prevention coin.* Eur Heart J, 2016. **37**(22): p. 1720-2.
3. Fisher, E.A., et al., *High-Density Lipoprotein Function, Dysfunction, and Reverse Cholesterol Transport.* Arteriosclerosis Thrombosis and Vascular Biology, 2012. **32**(12): p. 2813-2820.
4. Rohatgi, A., et al., *HDL cholesterol efflux capacity and incident cardiovascular events.* N Engl J Med, 2014. **371**(25): p. 2383-93.
5. Saleheen, D., et al., *Association of HDL cholesterol efflux capacity with incident coronary heart disease events: a prospective case-control study.* Lancet Diabetes Endocrinol, 2015. **3**(7): p. 507-13.
6. Rosenson, R.S., et al., *Dysfunctional HDL and atherosclerotic cardiovascular disease.* Nat Rev Cardiol, 2016. **13**(1): p. 48-60.
7. Feig, J.E., et al., *High-density lipoprotein and atherosclerosis regression: evidence from preclinical and clinical studies.* Circ Res, 2014. **114**(1): p. 205-13.
8. Siebel, A.L., S.E. Heywood, and B.A. Kingwell, *HDL and glucose metabolism: current evidence and therapeutic potential.* Front Pharmacol, 2015. **6**: p. 258.
9. Dalla-Riva, J., et al., *Discoidal HDL and apoA-I-derived peptides improve glucose uptake in skeletal muscle.* J Lipid Res, 2013. **54**(5): p. 1275-82.
10. Drew, B.G., et al., *High-density lipoprotein modulates glucose metabolism in patients with type 2 diabetes mellitus.* Circulation, 2009. **119**(15): p. 2103-11.
11. Barter, P.J., et al., *Effect of torcetrapib on glucose, insulin, and hemoglobin A1c in subjects in the Investigation of Lipid Level Management to Understand its Impact in Atherosclerotic Events (ILLUMINATE) trial.* Circulation, 2011. **124**(5): p. 555-62.
12. Shao, B.H., et al., *Oxidation of apolipoprotein A-I by myeloperoxidase impairs the initial interactions with ABCA1 required for signaling and cholesterol export.* Journal of Lipid Research, 2010. **51**(7): p. 1849-1858.
13. Huang, Y., et al., *An abundant dysfunctional apolipoprotein A1 in human atheroma.* Nat Med, 2014. **20**(2): p. 193-203.
14. Gonen, A., et al., *Atheroprotective immunization with malondialdehyde-modified LDL is hapten specific and dependent on advanced MDA adducts: implications for development of an atheroprotective vaccine.* J Lipid Res, 2014. **55**(10): p. 2137-55.
15. Busch, C.J. and C.J. Binder, *Malondialdehyde epitopes as mediators of sterile inflammation.* Biochim Biophys Acta, 2017. **1862**(4): p. 398-406.

16. Shanmugam, N., et al., *Proinflammatory effects of advanced lipoxidation end products in monocytes.* Diabetes, 2008. **57**(4): p. 879-88.
17. Shao, B., et al., *Modifying apolipoprotein A-I by malondialdehyde, but not by an array of other reactive carbonyls, blocks cholesterol efflux by the ABCA1 pathway.* J Biol Chem, 2010. **285**(24): p. 18473-84.
18. May-Zhang, L.S., et al., *Modification by isolevuglandins, highly reactive gamma-ketoaldehydes, deleteriously alters high-density lipoprotein structure and function.* J Biol Chem, 2018. **293**(24): p. 9176-9187.
19. Davies, S.S., et al., *Pyridoxamine analogues scavenge lipid-derived gamma-ketoaldehydes and protect against H2O2-mediated cytotoxicity.* Biochemistry, 2006. **45**(51): p. 15756-67.
20. Huang, J., F. Smith, and P. Panizzi, *Ordered cleavage of myeloperoxidase ester bonds releases active site heme leading to inactivation of myeloperoxidase by benzoic acid hydrazide analogs.* Arch Biochem Biophys, 2014. **548**: p. 74-85.
21. Huang, J., et al., *Inactivation of myeloperoxidase by benzoic acid hydrazide.* Arch Biochem Biophys, 2015. **570**: p. 14-22.
22. Linton, M.F., J.B. Atkinson, and S. Fazio, *Prevention of atherosclerosis in apolipoprotein E-deficient mice by bone marrow transplantation.* Science, 1995. **267**(5200): p. 1034-7.
23. Nicholls, S.J., et al., *Cholesterol Efflux Capacity and Pre-Beta-1 HDL Concentrations Are Increased in Dyslipidemic Patients Treated With Evacetrapib.* J Am Coll Cardiol, 2015. **66**(20): p. 2201-2210.
24. Khera, A.V., et al., *Cholesterol efflux capacity, high-density lipoprotein function, and atherosclerosis.* N Engl J Med, 2011. **364**(2): p. 127-35.
25. Robinet, P., et al., *A simple and sensitive enzymatic method for cholesterol quantification in macrophages and foam cells.* J Lipid Res, 2010. **51**(11): p. 3364-9.
26. Shea, S., et al., *Cholesterol Mass Efflux Capacity, Incident Cardiovascular Disease, and Progression of Carotid Plaque.* Arterioscler Thromb Vasc Biol, 2019. **39**(1): p. 89-96.
27. Furuhashi, M., et al., *Treatment of diabetes and atherosclerosis by inhibiting fatty-acid-binding protein aP2.* Nature, 2007. **447**(7147): p. 959-65.
28. Babaev, V.R., et al., *Loss of Rictor in Monocyte/Macrophages Suppresses Their Proliferation and Viability Reducing Atherosclerosis in LDLR Null Mice.* Front Immunol, 2018. **9**: p. 215.
29. Maessen, D.E., et al., *Delayed Intervention With Pyridoxamine Improves Metabolic Function and Prevents Adipose Tissue Inflammation and Insulin Resistance in High-Fat Diet-Induced Obese Mice.* Diabetes, 2016. **65**(4): p. 956-66.
30. Tao, H., et al., *Macrophage SR-BI mediates efferocytosis via Src/PI3K/Rac1 signaling and reduces atherosclerotic lesion necrosis.* J Lipid Res, 2015. **56**(8): p. 1449-60.
31. Merat, S., et al., *Western-type diets induce insulin resistance and hyperinsulinemia in LDL receptor-deficient mice but do not increase aortic atherosclerosis compared with normoinsulinemic mice in which similar plasma cholesterol levels are achieved by a fructose-rich diet.* Arterioscler Thromb Vasc Biol, 1999. **19**(5): p. 1223-30.
32. Swirski, F.K., et al., *Ly-6Chi monocytes dominate hypercholesterolemia-associated monocytosis and give rise to macrophages in atheromata.* J Clin Invest, 2007. **117**(1): p. 195-205.
33. Babaev, V.R., et al., *Macrophage deficiency of Akt2 reduces atherosclerosis in Ldlr null mice.* J Lipid Res, 2014. **55**(11): p. 2296-308.
34. Babaev, V.R., et al., *Loss of 2 Akt (Protein Kinase B) Isoforms in Hematopoietic Cells Diminished Monocyte and Macrophage Survival and Reduces Atherosclerosis in Ldl Receptor-Null Mice.* Arterioscler Thromb Vasc Biol, 2018: p. ATVBAHA118312206.

35. Kimball, A., et al., *Ly6C(Hi) Blood Monocyte/Macrophage Drive Chronic Inflammation and Impair Wound Healing in Diabetes Mellitus.* Arterioscler Thromb Vasc Biol, 2018. **38**(5): p. 1102-1114.
36. Berg, K.E., et al., *Elevated CD14++CD16- monocytes predict cardiovascular events.* Circ Cardiovasc Genet, 2012. **5**(1): p. 122-31.
37. Heine, G.H., et al., *CD14(++)CD16+ monocytes but not total monocyte numbers predict cardiovascular events in dialysis patients.* Kidney Int, 2008. **73**(5): p. 622-9.
38. Fadini, G.P., et al., *Pro-inflammatory monocyte-macrophage polarization imbalance in human hypercholesterolemia and atherosclerosis.* Atherosclerosis, 2014. **237**(2): p. 805-8.
39. Hjuler Nielsen, M., et al., *Elevated atherosclerosis-related gene expression, monocyte activation and microparticle-release are related to increased lipoprotein-associated oxidative stress in familial hypercholesterolemia.* PLoS One, 2015. **10**(4): p. e0121516.
40. Rogacev, K.S., et al., *CD14++CD16+ monocytes independently predict cardiovascular events: a cohort study of 951 patients referred for elective coronary angiography.* J Am Coll Cardiol, 2012. **60**(16): p. 1512-20.
41. Tie, G., et al., *Hypercholesterolemia induces oxidant stress that accelerates the ageing of hematopoietic stem cells.* J Am Heart Assoc, 2014. **3**(1): p. e000241.
42. Tall, A.R., et al., *Cholesterol efflux: a novel regulator of myelopoiesis and atherogenesis.* Arterioscler Thromb Vasc Biol, 2012. **32**(11): p. 2547-52.
43. Nahrendorf, M. and F.K. Swirski, *Abandoning M1/M2 for a Network Model of Macrophage Function.* Circ Res, 2016. **119**(3): p. 414-7.
44. Ridker, P.M., et al., *Antiinflammatory Therapy with Canakinumab for Atherosclerotic Disease.* N Engl J Med, 2017. **377**(12): p. 1119-1131.
45. Liu, C., et al., *Effects of a novel pharmacologic inhibitor of myeloperoxidase in a mouse atherosclerosis model.* PLoS One, 2012. **7**(12): p. e50767.
46. Huang, J., et al., *Methods for measuring myeloperoxidase activity toward assessing inhibitor efficacy in living systems.* J Leukoc Biol, 2016. **99**(4): p. 541-8.
47. Manchanda, K., et al., *MPO (Myeloperoxidase) Reduces Endothelial Glycocalyx Thickness Dependent on Its Cationic Charge.* Arterioscler Thromb Vasc Biol, 2018.
48. Daugherty, A., et al., *Myeloperoxidase, a catalyst for lipoprotein oxidation, is expressed in human atherosclerotic lesions.* J Clin Invest, 1994. **94**(1): p. 437-44.
49. van Leeuwen, M., et al., *Accumulation of myeloperoxidase-positive neutrophils in atherosclerotic lesions in LDLR-/- mice.* Arterioscler Thromb Vasc Biol, 2008. **28**(1): p. 84-9.
50. Boring, L., et al., *Decreased lesion formation in CCR2-/- mice reveals a role for chemokines in the initiation of atherosclerosis.* Nature, 1998. **394**(6696): p. 894-7.
51. Verweij, S.L., et al., *CCR2 expression on circulating monocytes is associated with arterial wall inflammation assessed by 18F-FDG PET/CT in patients at risk for cardiovascular disease.* Cardiovasc Res, 2018. **114**(3): p. 468-475.
52. Lee, M.K., et al., *High-density lipoprotein inhibits human M1 macrophage polarization through redistribution of caveolin-1.* Br J Pharmacol, 2016. **173**(4): p. 741-51.
53. Sanson, M., E. Distel, and E.A. Fisher, *HDL induces the expression of the M2 macrophage markers arginase 1 and Fizz-1 in a STAT6-dependent process.* PLoS One, 2013. **8**(8): p. e74676.
54. Yvan-Charvet, L., et al., *Increased inflammatory gene expression in ABC transporter-deficient macrophages: free cholesterol accumulation, increased signaling via toll-like receptors, and neutrophil infiltration of atherosclerotic lesions.* Circulation, 2008. **118**(18): p. 1837-47.

55. Zhu, X., et al., *Increased cellular free cholesterol in macrophage-specific Abca1 knock-out mice enhances pro-inflammatory response of macrophages.* J Biol Chem, 2008. **283**(34): p. 22930-41.
56. Han, R., et al., *Apolipoprotein A-I stimulates AMP-activated protein kinase and improves glucose metabolism.* Diabetologia, 2007. **50**(9): p. 1960-1968.
57. Song, P., et al., *Apolipoprotein a1 increases mitochondrial biogenesis through AMP-activated protein kinase.* Cellular Signalling, 2015. **27**(9): p. 1873-1881.
58. Marsche, G., et al., *Hypochlorite-modified high density lipoprotein, a high affinity ligand to scavenger receptor class B, type I, impairs high density lipoprotein-dependent selective lipid uptake and reverse cholesterol transport.* J Biol Chem, 2002. **277**(35): p. 32172-9.
59. Panzenboeck, U., et al., *Effects of reagent and enzymatically generated hypochlorite on physicochemical and metabolic properties of high density lipoproteins.* J Biol Chem, 1997. **272**(47): p. 29711-20.

Figure legend

Figure 1. PPM prevents MPO-mediated and MDA mediated HDL modification and preserves HDL cholesterol efflux capacity. A-B PPM prevents the crosslinking of apoAI on HDL caused by MDA modification. C, PPM preserves MDA-HDL cholesterol efflux capacity in Apoe$^{-/-}$ macrophages. D, PPM prevents MPO-mediated HDL modification and preserves HDL cholesterol efflux capacity. E, PPM improves the cholesterol efflux capacity of HDL in Ldlr$^{-/-}$ mice. F, PPM increases HDL associated atheroprotective enzyme PON1 activity in Ldlr$^{-/-}$ mice. Graphs represent data (mean ± SEM) of the experiments; *P <0.05 by T-test or one way ANOVA.

Figure 2. PPM reduces fast glucose, insulin levels and improves insulin sensitivity in male Ldlr$^{-/-}$ mice. A&B, PPM reduces fast glucose levels and reduces fast insulin levels in male Ldlr$^{-/-}$ mice. C, PPM normalizes HOMA-IR values in male Ldlr$^{-/-}$ mice. D&E, Effect of PPM on glucose changes in male Ldlr$^{-/-}$ mice in response to injection of glucose using IPGTT as mentioned in Methods (n=10 in each group). F&G, Effect of PPM on glucose changes in male Ldlr-/- mice in response to injection of insulin using IPITT as mentioned in Methods (n=10 in each group). H&I, Effect of PPM on hepatic fat deposition in Ldlr$^{-/-}$ mice was determined using H&E staining (n=6). Scale bar= 100 μm. A.U., arbitrary units. Graphs represent data (mean ± SEM) of the experiments; *P <0.05 by one way ANOVA.

Figure 3. PPM reduces atherosclerotic lesion and the macrophage content of lesion in female Ldlr$^{-/-}$ mice. A, B and C PPM does not affect cholesterol levels, triglyceride levels and lipid profile from FPLC fractions in female Ldlr$^{-/-}$ mice. D&E, PPM reduces the aortic root atherosclerotic lesions in female Ldlr$^{-/-}$ mice. Female Ldlr$^{-/-}$ mice were pretreated with 1 g/L of PPO or1 g/L of PPM for 2 weeks on chow diet. Then mice were treated with 1 g/L of PPM or1 g/L of PPO for 16 weeks on WD. Oil-Red-O staining of atherosclerotic lesion in female Ldlr$^{-/-}$ mice with PPO (n=12) or PPM (n=12). F&G, PPM reduces the macrophage content in lesions of female Ldlr$^{-/-}$ mice. Graphs represent data (mean ± SEM) of the experiments; *P <0.05, ** P<0.01, ***P<0.001 by one-way ANOVA.

Figure 4. PPM reduces aortic root atherosclerotic lesions and en face atherosclerotic lesions in male Ldlr$^{-/-}$ mice. A & B, PPM does not affect plasma cholesterol levels and triglyceride levels in male Ldlr$^{-/-}$ mice. C&D, PPM reduces the aortic root atherosclerotic lesions

in male Ldlr$^{-/-}$ mice. E&F, PPM reduces en face atherosclerotic lesion in male Ldlr$^{-/-}$ mice. Male Ldlr$^{-/-}$ mice were pretreated with 1 g/L of PPM for 2 weeks on chow diet. Then mice were treated with 1 g/L of PPM for 16 weeks on WD. Oil-Red-O staining of atherosclerosis lesion in male Ldlr$^{-/-}$ mice with vehicle (n=8) or PPM (n=10) is shown. Graphs represent data (mean ± SEM) of the experiments; *P <0.05, ** P<0.01, ***P<0.001 by T-test.

Figure 5. PPM increases Arg1 expression, reduces CCR2 expression and MPO expression in atherosclerotic lesions of Ldlr$^{-/-}$ mice. A, immunohistochemistry staining of CCR2+ macrophages was performed as mentioned in Methods. B, PPM reduces the number of CCR2+ macrophages in lesions of Ldlr$^{-/-}$ mice. C&D. Immunohistochemistry staining of Arg1+ macrophages was performed as mentioned in Methods. D, PPM increases the number of Arg1+ macrophages in lesions of Ldlr$^{-/-}$ mice. E. Pro-inflammatory enzyme MPO staining of atherosclerotic lesions in Ldlr$^{-/-}$ mice is shown. F, PPM reduces MPO expression in atherosclerotic lesions of Ldlr$^{-/-}$ mice. Scale bar = 20 μm. n=6 in each group, Graphs represent data (mean ± SEM) of the experiments; *P <0.05 by T-test.

Figure 6. PPM reduces the number of apoptotic cells and the MDA content in lesions of Ldlr$^{-/-}$ mice. A, MOMA2+ macrophages staining and TUNEL positive staining of atherosclerotic lesions in male Ldlr$^{-/-}$ mice are shown. B, PPM reduces the apoptotic cells in atherosclerotic lesions of male Ldlr$^{-/-}$ mice (n=6). C & D, PPM reduces the MDA-HDL, MDA-LDL content in Ldlr$^{-/-}$ mice on WD for 16 weeks. E & F, PPM reduces the content of MDA of Ldlr$^{-/-}$ mice (n=3). G, PPM reduces the IL-1β levels of Ldlr$^{-/-}$ mice (n=7-8). Scale bar = 20 μm. Graphs represent data (mean ± SEM) of the experiments; *P <0.05 by T-test.

Figure 7. PPM stabilizes the atherosclerotic plaque in Ldlr$^{-/-}$ mice. A, the plaque stability was measured by using Trichrome staining of atherosclerotic lesions of Ldlr$^{-/-}$ mice (n=6 in each group). B, C and D, collagen content (blue staining area), fibrous cap thickness and necrotic area were quantified from atherosclerotic lesions of Ldlr-/- mice (n=6 in each group). Scale bar = 40um. Graphs represent data (mean ± SEM) of the experiments; *P <0.05 by T-test.

Figure 8. PPM decreases the number of Ly6C^{hi} monocytes and ratio of Ly6C^{hi} to Ly6c^{Low} monocytes in Ldlr$^{-/-}$ mice. A-B, the representative flow cytometry gating strategies for monocyte subsets, neutrophils, T cell, B cells in peripheral blood of Ldlr$^{-/-}$ mice are shown. C-F, PPM does not affect the number of neutrophils, Ly6 ^{low} monocytes, but reduces the number of Ly6C^{hi} monocytes and the ratio of Ly6C^{hi} to Ly6C ^{low} monocytes in female Ldlr$^{-/-}$ mice (n=9 in each group) on western diet for 14 weeks. Graphs represent data (mean ± SEM) of the experiments; *P <0.05 by T-test.

Fig 1

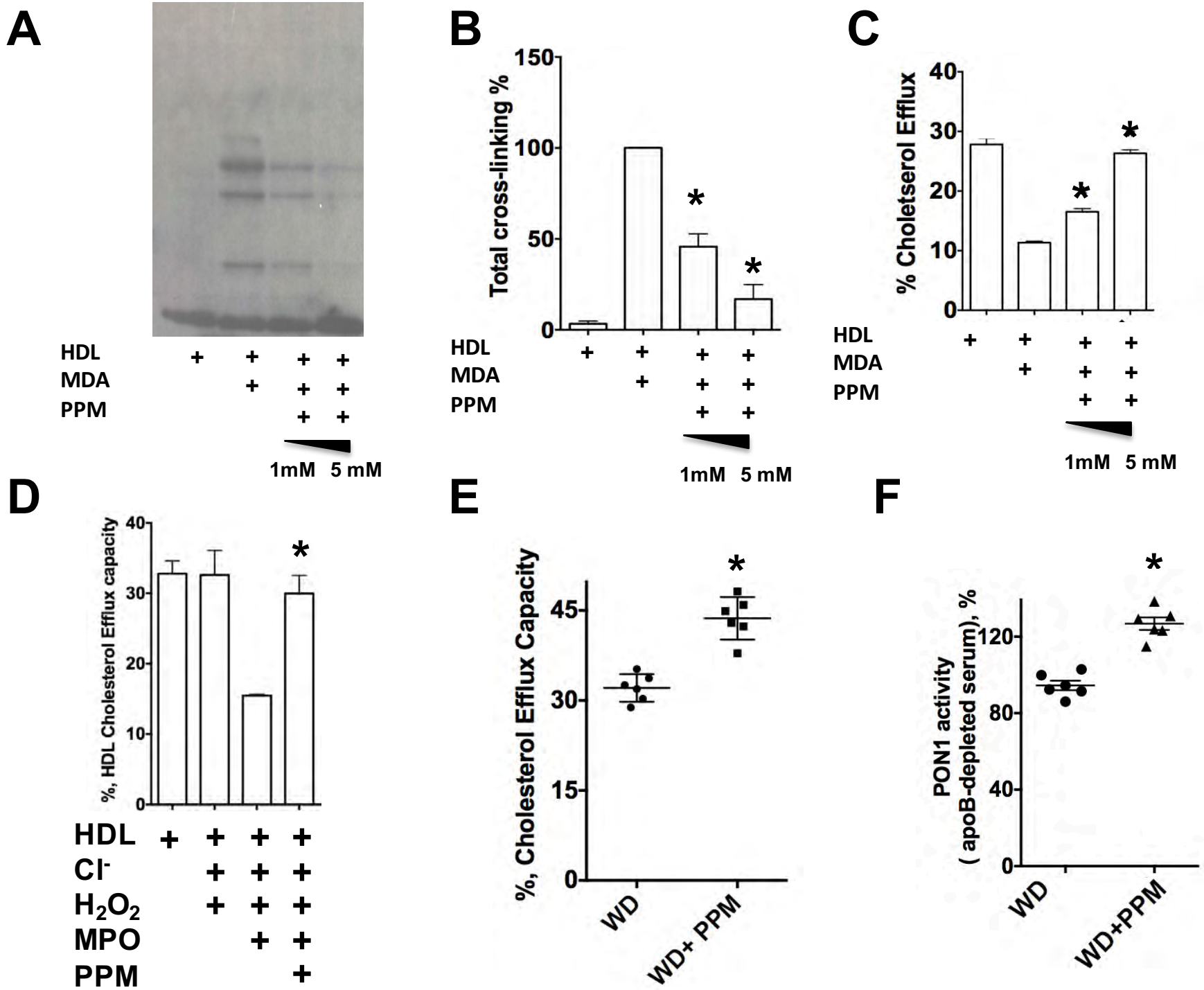
A
HDL
MDA
PPM
1mM 5 mM
B
Total cross-linking %
150
100
50
0
HDL
MDA
PPM
1mM 5 mM
C
% Choletserol Efflux
40
30
20
10
0
HDL
MDA
PPM
1mM 5 mM
D
%, HDL Cholesterol Efflux capacity
40
30
20
10
0
HDL
Cl-
H2O2
MPO
PPM
E
%, Cholesterol Efflux Capacity
45
30
15
0
WD
WD+ PPM
F
PON1 activity
(apoB-depleted serum), %
120
80
40
0
WD
WD+PPM

Fig 2

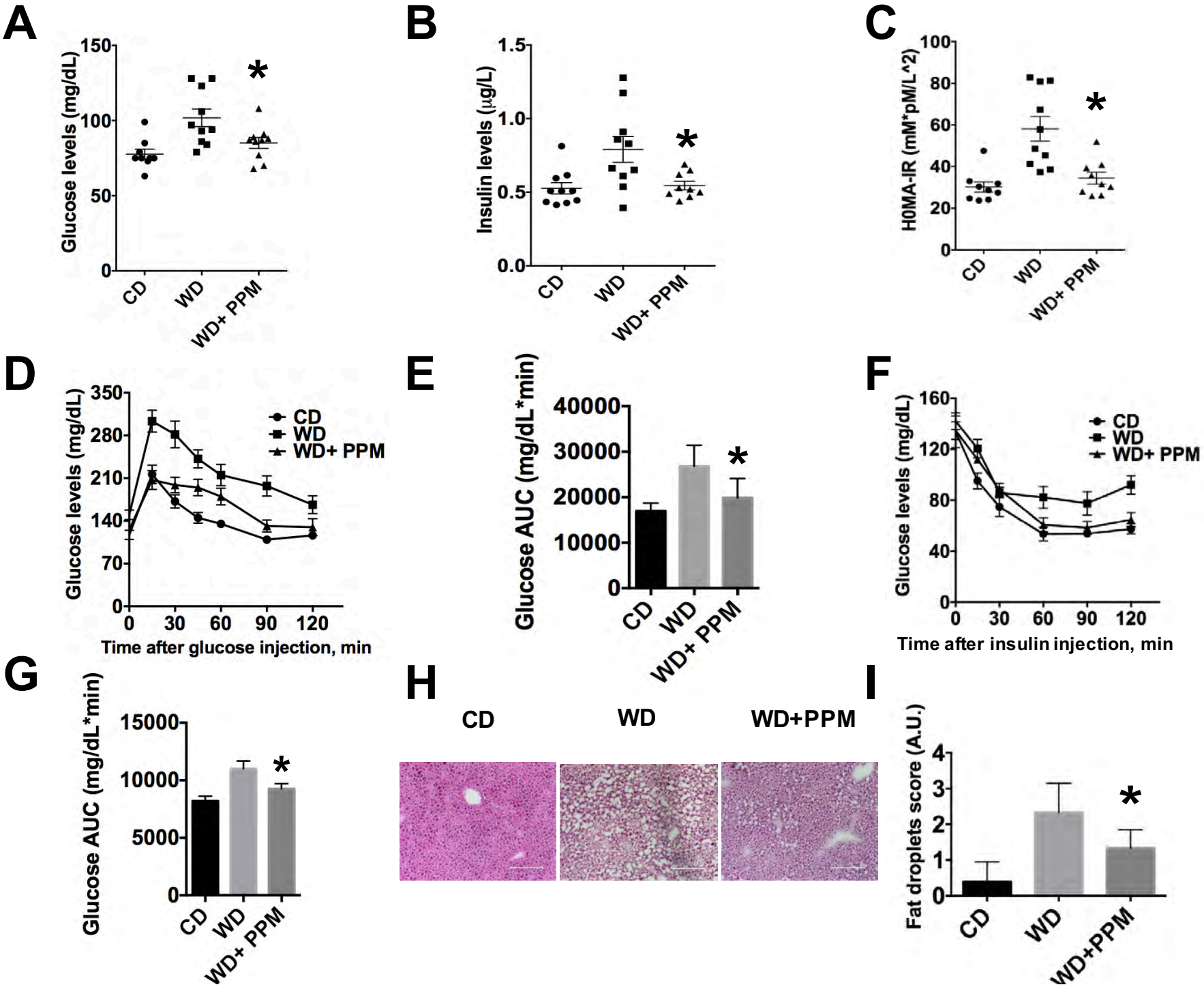
A
Glucose levels (mg/dL)
150
100
50
0
CD
WD
WD+ PPM
*
B
Insulin levels (μg/L)
1.5
1.0
0.5
0.0
CD
WD
WD+ PPM
*
C
H0MA-IR (mM*pM/L^2)
100
80
60
40
20
0
CD
WD
WD+ PPM
*
D
Glucose levels (mg/dL)
350
280
210
140
70
0
0
30
60
90
120
Time after glucose injection, min
CD
WD
WD+ PPM
E
Glucose AUC (mg/dL*min)
40000
30000
20000
10000
0
CD
WD
WD+ PPM
*
F
Glucose levels (mg/dL)
160
120
80
40
0
0
30
60
90
120
Time after insulin injection, min
CD
WD
WD+ PPM
G
Glucose AUC (mg/dL*min)
15000
10000
5000
0
CD
WD
WD+ PPM
*
H
CD
WD
WD+PPM
I
Fat droplets score (A.U.)
4
3
2
1
0
CD
WD
WD+PPM
*

Fig 3

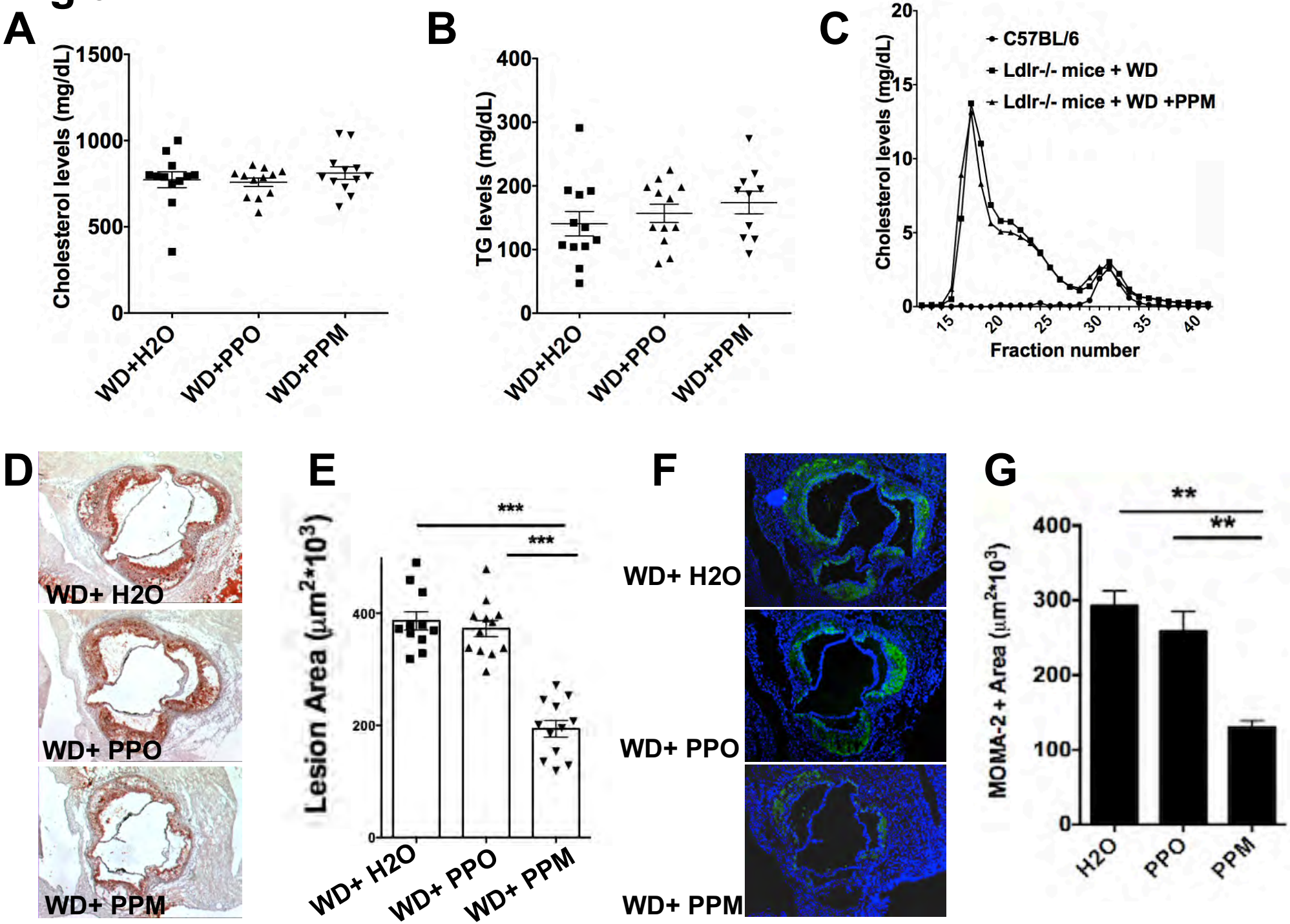
A
Cholesterol levels (mg/dL)
1500
1000
500
0
WD+H2O
WD+PPO
WD+PPM
B
TG levels (mg/dL)
400
300
200
100
0
WD+H2O
WD+PPO
WD+PPM
C
Cholesterol levels (mg/dL)
20
15
10
5
0
C57BL/6
Ldlr-/- mice + WD
Ldlr-/- mice + WD +PPM
15
20
25
30
35
40
Fraction number
D
WD+ H2O
WD+ PPO
WD+ PPM
E
Lesion Area (μm2*10^3)
***
***
400
200
0
WD+ H2O
WD+ PPO
WD+ PPM
F
WD+ H2O
WD+ PPO
WD+ PPM
G
MOMA-2 + Area (μm2*10^3)
**
**
400
300
200
100
0
H2O
PPO
PPM

Fig 4

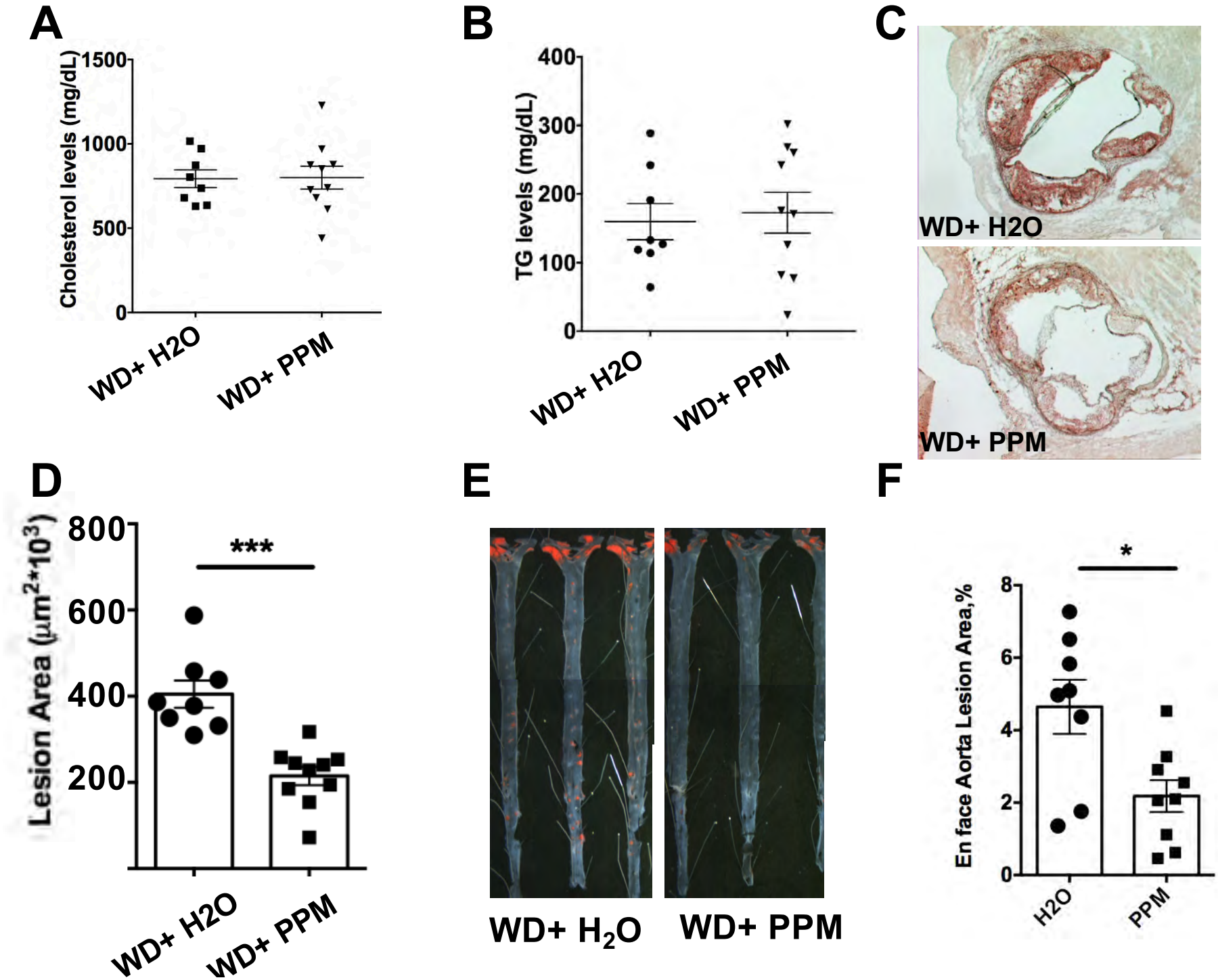
A
Cholesterol levels (mg/dL)
1500
1000
500
0
WD+ H2O
WD+ PPM
B
TG levels (mg/dL)
400
300
200
100
0
WD+ H2O
WD+ PPM
C
WD+ H2O
WD+ PPM
D
Lesion Area (µm2*10³)
800
600
400
200
***
WD+ H2O
WD+ PPM
E
WD+ H2O
WD+ PPM
F
En face Aorta Lesion Area,%
8
6
4
2
0
*
H2O
PPM

Fig 5

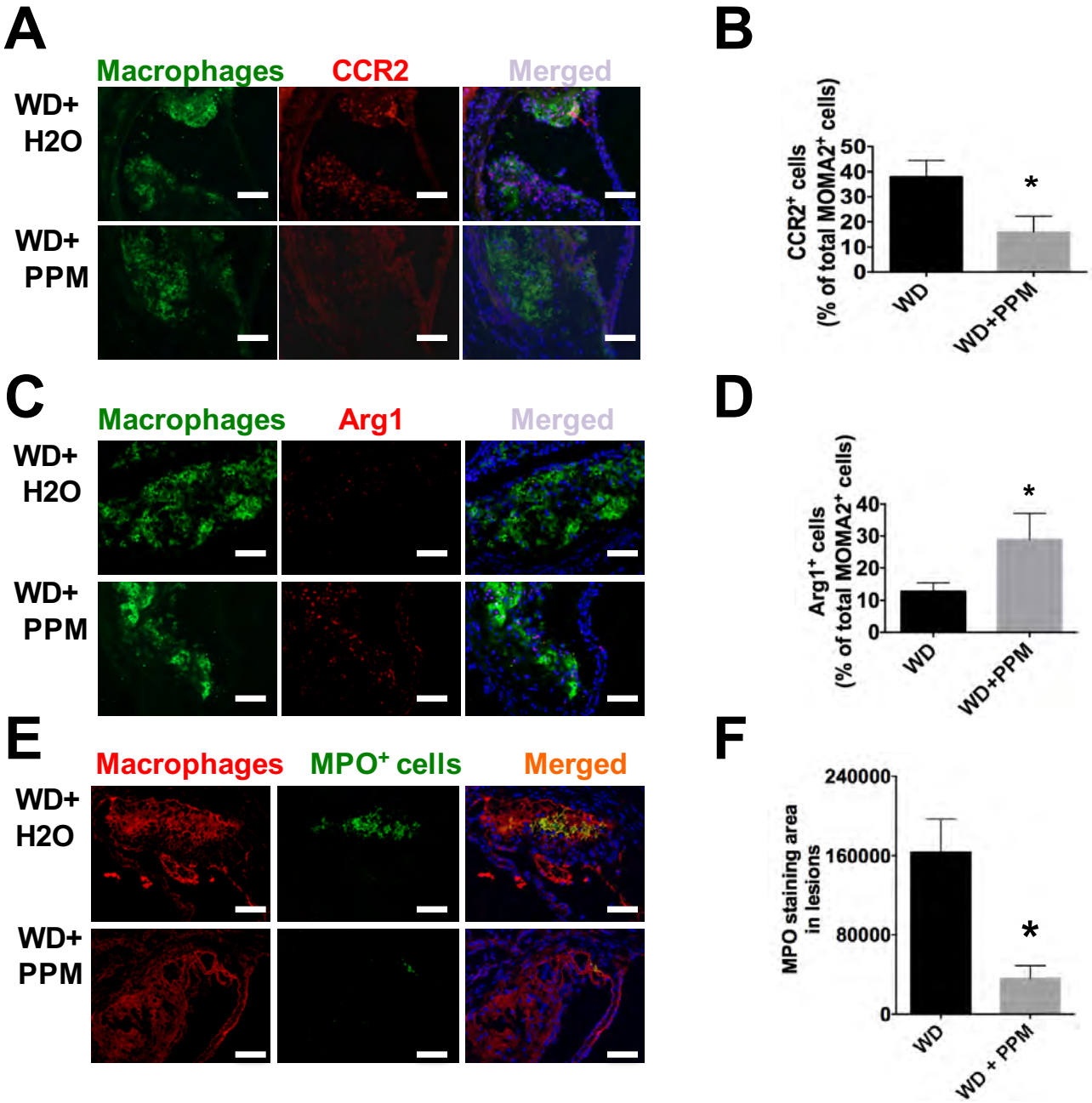
A
Macrophages
CCR2
Merged
WD+ H2O
WD+ PPM
B
CCR2+ cells (% of total MOMA2+ cells)
50
40
30
20
10
0
*
WD
WD+PPM
C
Macrophages
Arg1
Merged
WD+ H2O
WD+ PPM
D
Arg1+ cells (% of total MOMA2+ cells)
40
30
20
10
0
*
WD
WD+PPM
E
Macrophages
MPO+ cells
Merged
WD+ H2O
WD+ PPM
F
MPO staining area in lesions
240000
160000
80000
0
*
WD
WD + PPM

Fig 6

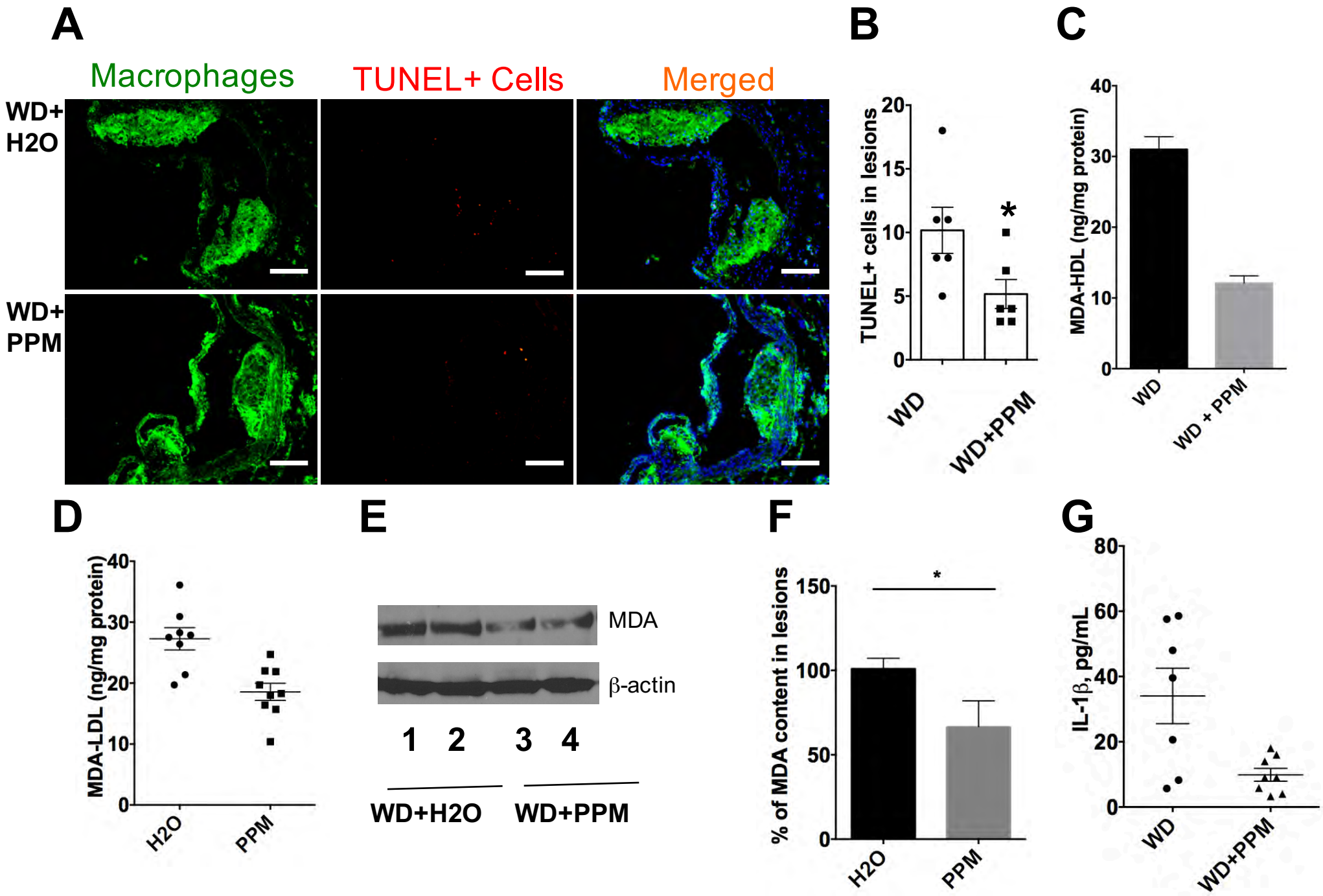
A
Macrophages
TUNEL+ Cells
Merged
WD+ H2O
WD+ PPM
B
TUNEL+ cells in lesions
20
15
10
5
0
*
WD
WD+PPM
C
MDA-HDL (ng/mg protein)
40
30
20
10
0
WD
WD + PPM
D
MDA-LDL (ng/mg protein)
40
30
20
10
0
H2O
PPM
E
MDA
β-actin
1 2 3 4
WD+H2O
WD+PPM
F
% of MDA content in lesions
150
100
50
0
*
H2O
PPM
G
IL-1β, pg/mL
80
60
40
20
0
WD
WD+PPM

Fig 7

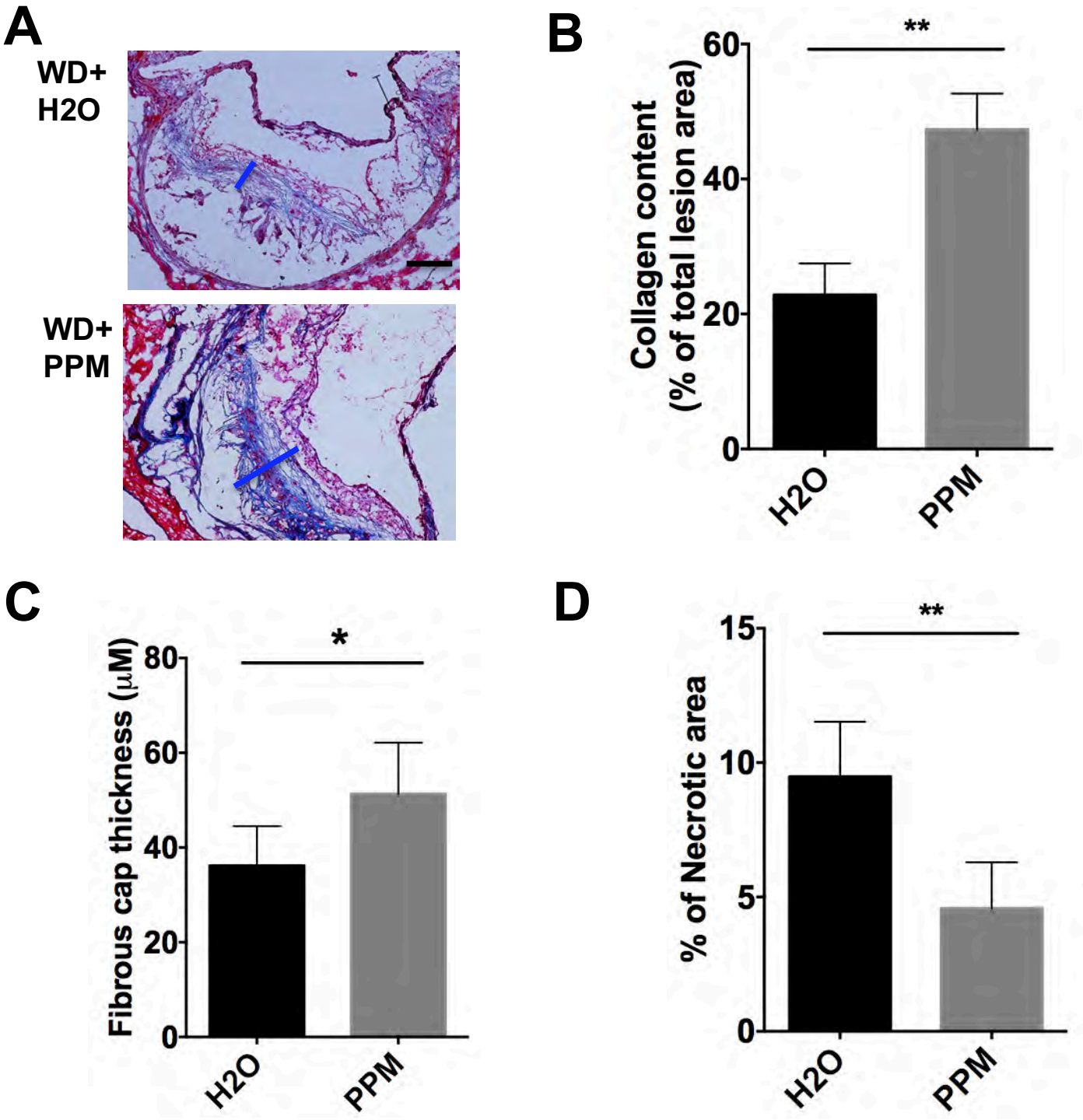
A
WD+
H2O
WD+
PPM
B
Collagen content
(% of total lesion area)
60
40
20
0
**
H2O
PPM
C
Fibrous cap thickness (μM)
80
60
40
20
0
*
H2O
PPM
D
% of Necrotic area
15
10
5
0
**
H2O
PPM

Fig 8

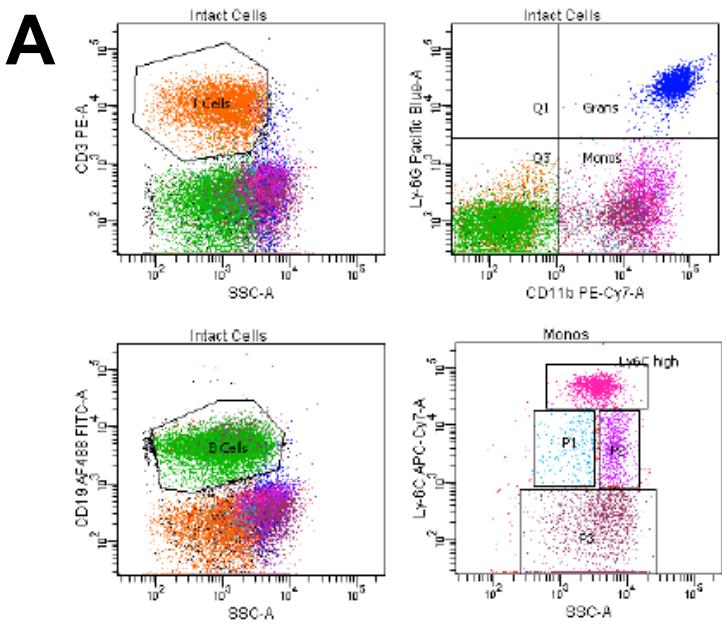

Ldlr$^{-/-}$ mice

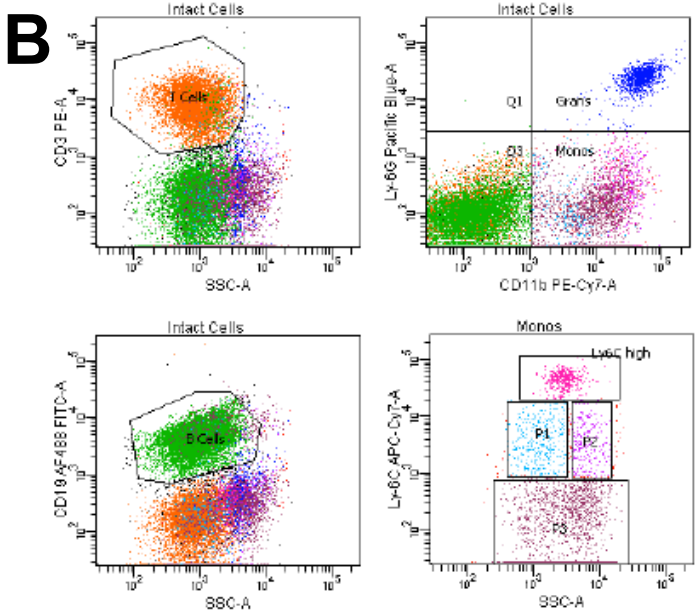
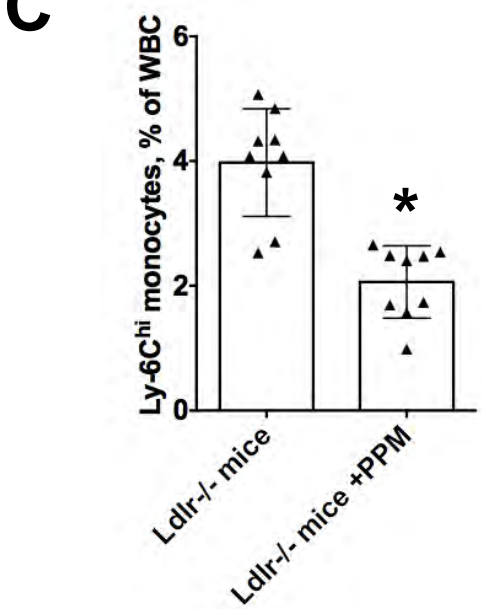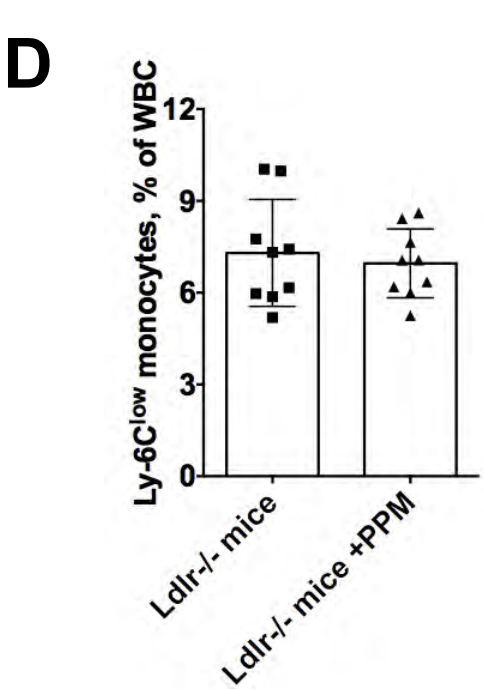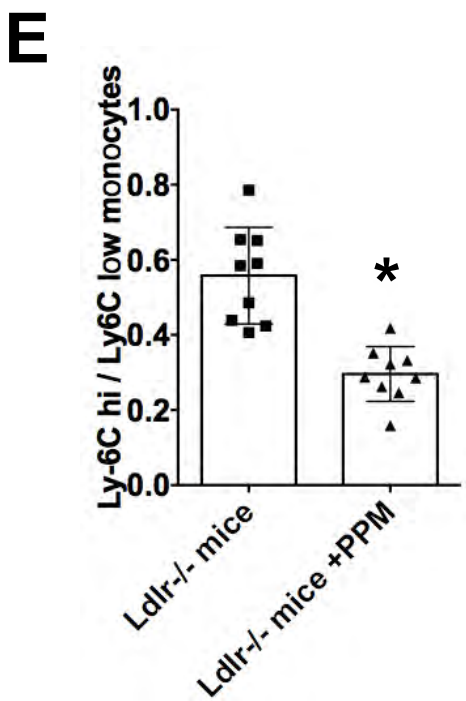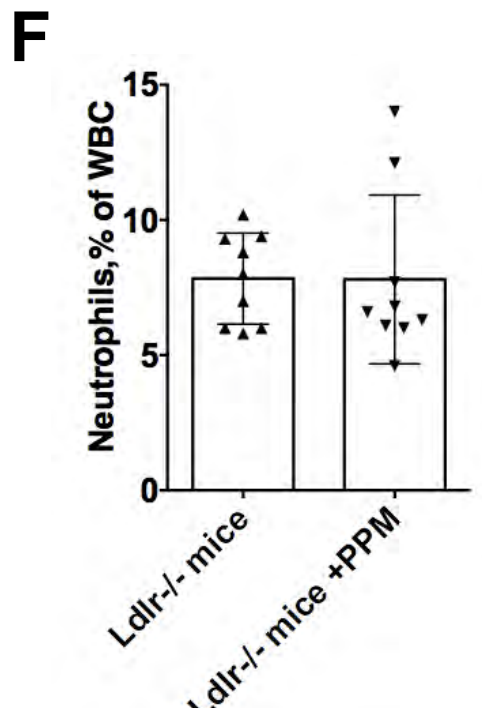
Ldlr$^{-/-}$ mice + PPM